Istraživanja i projektovanja za privredu
ISSN 1451-4117
DOI:10.5937/jaes0-44991
www.engineeringscience.rs

iipp publishing

Journal of Applied Engineering Science
Vol. 22, No. 1, 2024
Original Scientific Paper
Paper number: 22(2024)1, 1169, 81-88

RESEARCH AND DESIGN OF AN EFFICIENT ADAPTIVE DRIVE WITH BALANCING FRICTION COUPLING

Kuanysh Alipbayev, Konstantin Ivanov, Aidos Sultan*, Arman Komekbayev

Telecommunications and Innovative Technologies department, Almaty University of Power Engineering and Telecommunications named after Gumarbek Daukeyev, Kazakhstan

** aiiddoss17@mail.ru*

Currently, research related to the automation of processes, systems and devices are of high relevance in the scientific and technical field: in the aerospace industry, robotics and electric transport technology. Successful automation of facilities and processes requires simplified control systems, and an adaptive mechanical system operates without a control system, which increases its reliability and efficiency. In particular, the creation of an efficient and reliable transmission of electric autonomous and mobile vehicles can be achieved by an adaptive mechanical drive with two degrees of freedom. Adaptation of the two-mobile system (2-DoF) is achieved by the proposed completely new type of transmission, namely the design of a stepless multi-speed drive with an additional friction coupling. The property of reliable adaptation of a two-mobile self-adjusting mechanical drive is independent adaptability to an external load with the help of a balancing friction coupling that provides a connection between the frictional moment and the relative angular velocity. The article presents a study of the interaction of the parameters of a two- mobile system in order to improve the efficiency of a self-adjusting adaptive drive with a given wide range of regulation based on the use of a friction coupling.

Keywords: self-adjusting adaptive drive, additional constraint, friction coupling, friction moment, regulatory efficiency

1 INTRODUCTION

The creation of modern automatically controlled drives is based on the improvement of multi-stage CVT designs. With the development of mechatronics technology, various new drives are used in drive systems to improve transmission efficiency [1]. There is a tendency to reduce the number of steps while maintaining a wide control range. To improve the efficiency of drive systems of mobile robots and electric vehicles, the use of multi-speed transmissions is widely studied [2].

Multi-speed gearboxes have been explored for application in the transmission of battery electric vehicles, since multiple ratios add the ability to keep the electric motor running in a higher efficiency area, thereby reducing vehicle energy consumption and improving dynamic performance [3].

The use of a multi-stage gearbox increases the cost of producing an electric vehicle and requires the introduction of a gearbox control [4] and the development of a gear shift algorithm [5].

Researchers have shown that multi-speed transmissions can reduce a vehicle's overall energy consumption, which can be translated into increased range with a smaller battery pack, improved dynamic performance and climbing ability. However, the efficiency of a conventional multi-stage gearbox is usually lower than that of a single-stage gearbox [6].

Recent studies have shown that multi-ratio systems can reduce energy consumption by 2 to 20% for various driving cycles [5], [6], [7] and increase drive wheel torque by 35% [8], although this results in to a decrease in efficiency.

For heavy-duty vehicles that, due to their mass, need very high torque for acceleration, multi-speed gearboxes may be more necessary so that a machine with lower torque and less tractive effort can be used [9].

The results of «Development of a Multi-Speed Dual Clutch CVT for Electric Vehicles» show that electric vehicles can gain significant range advantages from multi-speed transmissions. CVT shows the greatest potential and is one of the most promising transmissions for electric vehicles [10]. However, the use of a double clutch or other auxiliary control devices complicates the design of the drive and reduces efficiency.

It was noted in [11] that adaptive transmission control can be used to further improve the adaptability to working conditions and the economy of the vehicle. However, this also leads to a more complex design.

The paper [12] proposes a dual motor configuration in which two smaller motors are connected via a planetary gear, as opposed to the standard configuration which uses a single larger motor directly connected to the drive wheels with a fixed ratio reduction gear. The main disadvantage of this configuration is the problem of additional unsprung mass due to the twin-motor design, which degrades the dynamic performance of the electric vehicle. Also, the investigated multi-speed twin-engine transmission is not suitable for driving in unprepared terrain, since this type of configuration was only effective at low speeds and high torques. The dual motor drive system requires the use of a control, which also complicates the design.

The paper [13] proposes a two-speed automatic manual transmission with a selectable one-way clutch. The developed drive consists of a high-speed motor and a mechanical switching drive, and can carry out switching without interrupting the energy flow. The main disadvantage of the studies performed is that the automatically controlled drive

is built based on the use of single-mobile mechanical elements connected by a control system. As a result, a most complex controlled electromechanical system is created, which has a low adequacy to a changing external load and low efficiency.

On the above grounds, to create an efficient, compact system and an automatically controlled drive, it is proposed to use a previously developed adaptive mechanical system with two degrees of freedom without a control system [14].

The self-adjusting adaptive drive [15] is fundamentally different from all the drives considered above in that it provides effective overcoming of the resistance torque in a given wide range due to the use of two degrees of freedom. In this case, the definability of the motion of a two-mobile system with one input is achieved by introducing an additional constraint that ensures the replacement of the emerging unbalanced force by the calculated moment of resistance. Additional constraint is achieved by using a friction joint with a replacement moment of resistance. However, the mechanical transducer in the form of a friction joint used in the scheme under consideration turns out to be not a structural element due to large geometric parameters (trunnion radius) that do not correspond to the scheme.

The article presents a study of the interaction of the parameters of a two-mobile system in order to increase the efficiency of a self-adjusting adaptive drive with a given wide range of regulation based on the use of a balancing friction coupling.

The rest of the structure of this article is organized as follows: Section 2 describes the adaptive drive kinematics. Section 3 presents an optimization algorithm for obtaining optimal kinematic and power parameters of an adaptive drive. In section 4, a numerical calculation of the kinematic and power parameters of an adaptive drive is carried out with the determination of the efficiency. Section 5 analyzes the obtained results. Section 6 presents the main conclusions. Finally, the source of financing is presented in section 7.

2 DESCRIPTION OF THE KINEMATIC CHAIN OF THE ADAPTIVE DRIVE

An adaptive drive (hereinafter AD) is a self-adjusting mechanism (Fig. 1). The drive realizes the effect of power adaptation: the speed of the output link is inversely proportional to the variable output load. It has two degrees of freedom and only one input, which contradicts the condition for the existence of the mechanism and the definability of its motion. It was assumed that the definability of motion creates the necessary and sufficient conditions for power adaptation [15]. A necessary condition is provided by a movable closed loop made up of gears. The sufficient condition provides an additional constraint between force and velocity.

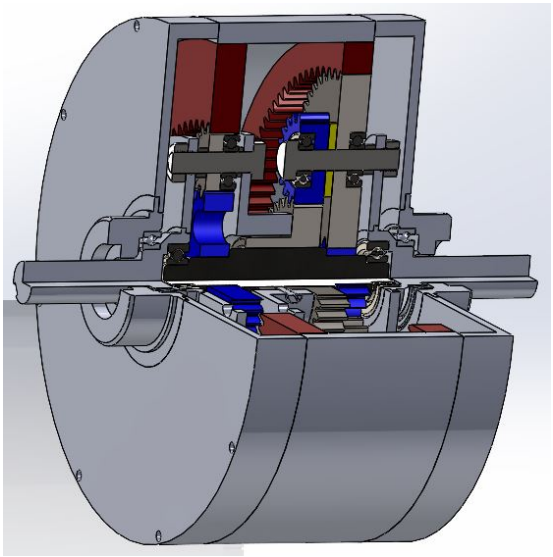

Fig. 1. 90-degree section view of an adaptive drive

The kinematic chain of the adaptive gear variator (Fig. 2a) contains a rack 0, an input carrier H_1, a closed loop of gears 1-2-3-6-5-4 and an output carrier H_2. Gear wheels 1, 2, 3, 6, 5, 4 form a movable closed loop with dynamic linkage. Gears 8, 7 form an additional parallel transmission from the carrier H_2 to the satellite 5. The closed loop contains an input satellite 2, a block of sun wheels 1-4, a block of ring wheels 3-6 and an output satellite 5.

Drive works as follows: the input shaft with the input carrier H_1 transmits the movement to the input satellite 2. Input satellite 2 transmits motion to gear blocks 1-4 and 3-6. Wheel blocks 1-4 and 3-6 transmit the movement to the output satellite 5 and the output carrier H_2. At the same time, a kinematic chain with an additional parallel transmission of gears 8-7 transmits the movement from the input carrier H_1 to the output satellite 5 and the carrier H_2. Parallel gear 8-7 has a gear ratio equal to the gear ratio of the planetary kinematic chain.

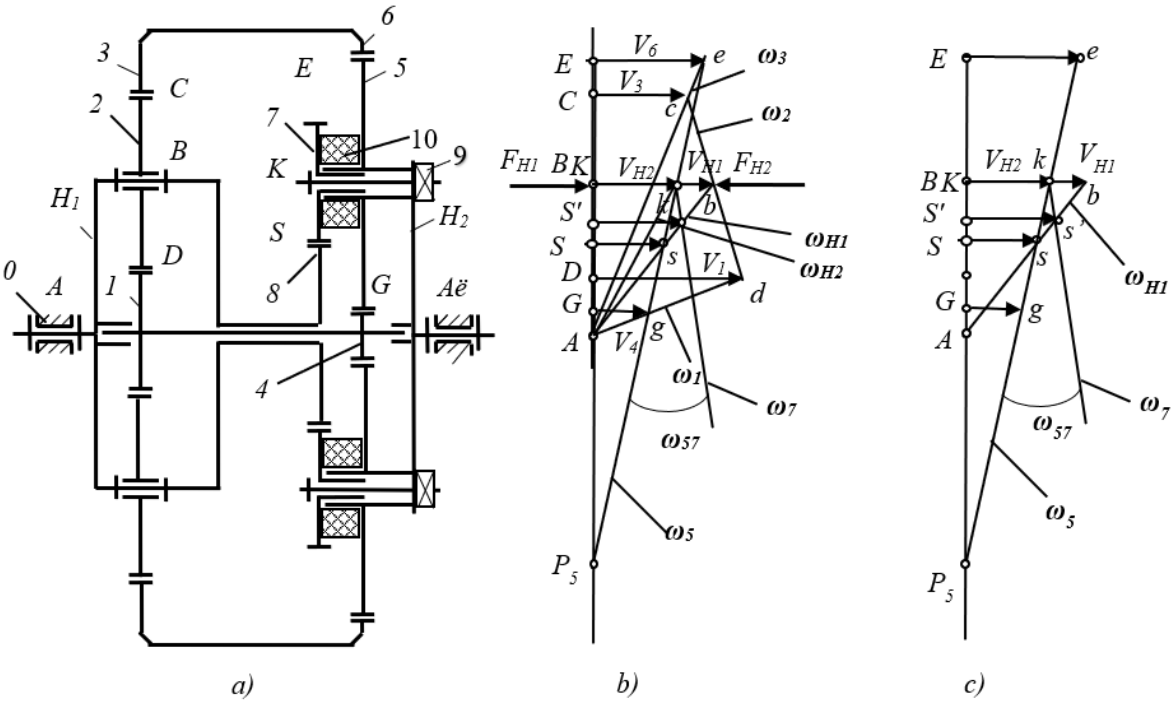

Fig. 2. Adaptive drive (a), plan of linear velocities of drive (b), determination of relative angular velocity (c)

Parallel gear 8-7 can create an effective force-velocity constraint. In the present work, the creation of force-velocity constraint by means of an adjustable friction coupling 10 connecting wheels 5 and 7 using an adjustable tension screw 9 is given. The tensioning screw 9 creates a normal reaction and frictional moment in the coupling 10 required for equilibration.

Figure 2c shows a simplified plan of linear velocities for easier visual perception.

Figure 3 shows a structural description of a 3D model of an adaptive drive.

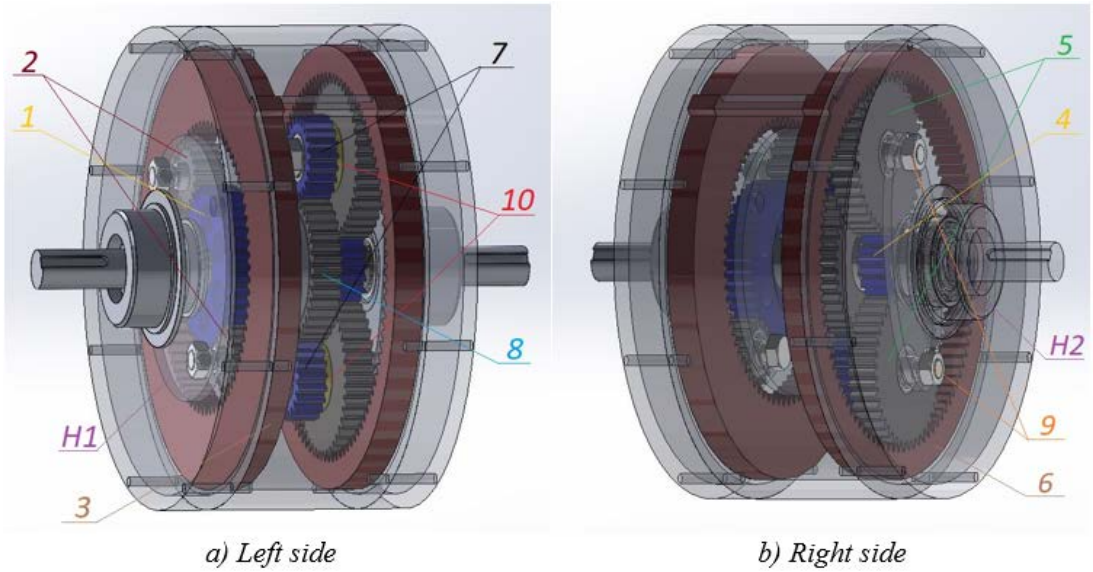

Fig. 3. Structural description of a 3D model of an adaptive drive:

1-4 – sun gears, 2 – driven gears, 3-6 – ring gears, 5 – driven gears, 7 – driven gears, 8 – sun gear, 9 – tension screw, 10 – friction coupling

3 KINEMATIC ANALYSIS OF ADAPTIVE DRIVE

The interaction of kinematic and force parameters will be represented in the form of a power balance and performed according to the principle of virtual works using actual displacements.

The interaction parameters are: external forces F_H1 and F_H2 (corresponding to moments 〖M〗_H1 and 〖M〗_H2) acting on the closed loop at points B and K , angular velocities 〖ω〗_H1, 〖ω〗_(H2) of the initial links , and linear velocities 〖V〗_H1, 〖V〗_H2 of points B and K (Fig. 2b, 2c).

The previously developed equations of interaction between the kinematic and power parameters [15] define a mathematical model of the adaptive drive without additional constraint.

The necessary condition for adaptation is provided by a movable closed loop composed of gear wheels. The closed loop equilibrium condition (without gear 8-7) is:

$$M_{H1}\omega_{H1} + M_{H2}\omega_{H2} = 0. \quad (1)$$

Eq. (1) allows us to obtain the necessary power adaptation condition, taking into account the negative sign of the output power:

$$\omega_{H2} = \frac{M_{H1} \cdot \omega_{H1}}{M_{H2}}. \quad (2)$$

The effect of power adaptation is as follows: for a given constant input power M_{H1}, ω_{H1} and a given output drag torque M_{H2}, the output angular velocity ω_{H2} is in inverse proportion to the variable output drag torque M_{H2}.

The necessary condition for adaptation expresses the theoretical possibility of creating an adaptation. The real adaptation can only take place if an additional sufficient adaptation condition is met.

A sufficient condition provides an additional constraint of force to velocity. The additional constraint is expressed by the Eq. of power consumption for friction in the friction coupling 10:

$$P_f = |M_f\omega_{75}|. \quad (3)$$

Here M_f – is the required frictional torque $M_f = Nf\rho$,

N – the normal reaction created by the tension screw 9,

f – coefficient of friction,

ρ – radius of the joint.

ω_{75} – the relative angular velocity of links 7 and 5.

The sufficient condition for power adaptation is represented by the power balance equation with the addition of power consumed by friction.

The power balance for a kinematic chain with additional frictional parallel constraint is as follows:

$$M_{H1}\omega_{H1} = M_{H2}\omega_{H2} + M_f\omega_{75}. \quad (4)$$

Force adaptation Eq.:

$$\omega_{H2} = \frac{M_{H1}\omega_{H1} - M_f\omega_{75}}{M_{H2}}. \quad (5)$$

The required friction torque can be pre-determined using the Eq. $M_f = -M_{H1}\frac{z_7}{z_8}$ with further refinement.

Eq. (5) eventually determines the mathematical model of the adaptive drive when the necessary and sufficient condition for force adaptation is met.

The values of angular velocities ω_5 and ω_7 are determined as follows:

1) For planetary gear:

$$\omega_5 = \omega_{H2} + (\omega_3 - \omega_{H2})u_{56}^{H2}. \quad (6)$$

2) For an additional gear:

$$\omega_7 = \omega_{H2} + (\omega_{H1} - \omega_{H2})u_{7-H1}^{H2}. \quad (7)$$

The relative angular velocity ω_{75} is determined by the Eq.:

$$\omega_{75} = \omega_7 - \omega_5. \quad (8)$$

The efficiency of the mechanism is determined by the Eq.:

$$\eta = \frac{P_{H1} - P_f}{P_{H1}} \cdot 100\%. \quad (9)$$

4 NUMERICAL CALCULATION OF THE MATHEMATICAL MODEL OF THE ADAPTIVE DRIVE

Numerical calculation of the mathematical model of the drive makes it possible to simply and quickly check the theoretical assumptions put forward. Let's analyze the drive operation by numerical analysis of the developed mathematical models:

1) AD-1 model corresponding to the necessary and sufficient condition of power adaptation [15].

2) AD-2 model corresponding to the approximate-sufficient condition of power adaptation, where ω_75=const.
3) AD-3 model corresponding to the real-sufficient condition of power adaptation, where ω_75≠const.

As an example, let's define the parameter values for one of the calculation options.

Initial data:

The adaptive drive has the given constant motor power parameters ω_{H1}, M_{H1} on the input link $H_1$and the given value of variable output torque resistance M_{H2} on the output link H_2 (figure 2a).

It is required to determine the power and kinematic parameters of the drive.

Model №1.

Given: ω_{H1} = 100 s^{-1}, M_{H1} = 10 *Nm*,

M_{H2}= [10, 15, 20, 25, 30, 35, 40, 45, 50] *Nm*,

M_{fK} = 4 *Nm*,

z_1 = 40; z_2 = 16; z_3 = 72; z_4 = 16; z_5 = 40; z_6 = 96.

Determine:

ω_5, ω_{5-H2}, P_{fK}, ω_{H2fK} and ɳ.

Solution:

Using Eq. (2), calculate the output angular velocity ω_{H2}.

The obtained data are summarized in Table 1.

Table 1: Values of output drag torque and output angular velocity for AD-1 with necessary condition of power adaptation

M_{H2}, Nm	10	15	20	25	30	35	40	45	50
ω_{H2}, s^{-1}	100,0	66,7	50,0	40,0	33,3	28,6	25,0	22,2	20,0

Table 1 values correspond to the necessary condition of power adaptation. To determine a sufficient condition of power adaptation, it is necessary to solve the following task.

Next, we define the values ω_5, ω_{5-H2}, P_{fK}, ω_{H2fK} and ɳ.

As an example, let's calculate the required parameters for M_{H2} = 10*Nm* and corresponding ω_{H2} = 100s^{-1}.

Power balance of kinematic chain with friction joint *K*:

$M_{H1}\omega_{H1} = M_{H2}\omega_{H2} + M_{fK}\omega_{5-H2}$,

where $\omega_{5-H2} = \omega_5 - \omega_{H2} = 100\ s^{-1} - 100s^{-1} = 0\ s^{-1}$.

Here $\omega_5 = \omega_{H2} + (\omega_3 - \omega_{H2})u_{56}^{H2} = 100 + (100 - 100) \cdot 2{,}4 = 100\ s^{-1}$,

where $\omega_3 = \frac{\omega_{H2}(1-u_{46}^{H2}) - \omega_{H1}(1-u_{13}^{H1})}{u_{13}^{H1} - u_{46}^{H2}} = \frac{100(1-(-6)) - 100(1-(-1{,}8))}{-1{,}8-(-6)} = 100\ s^{-1}$,

Let's determine the value of the frictional power P_{fK} using the following Eq.:

$P_{fK} = |M_{fK} \cdot \omega_{5-H2}| = |4\ Nm \cdot 0\ s^{-1}| = 0\ Nm.$

Let's determine the value of the output angular velocity ω_{H2fK} using the following Eq.:

$\omega_{H2fK} = \frac{M_{H1}\omega_{H1} - P_{fK}}{M_{H2}} = \frac{100\ Nm \cdot 10s^{-1} - 0\ Nm}{10\ Nm} = 100\ s^{-1}$.

Let's determine the value of the efficiency of the mechanism according to the following Eq.:

$ɳ = \frac{P_{H1} - P_{fK}}{P_{H1}} \cdot 100\% = \frac{1000\ Nm - 0\ Nm}{1000\ Nm} \cdot 100\% = 100\%.$

According to this solution algorithm, we determine the remaining parameters that determine the sufficient condition of power adaptation at the corresponding values of M_{H2} and ω_{H2} from Table 1. The obtained data are summarized in Table 2.

Table 2: Results of calculations for AD-1 with a sufficient condition of power adaptation

M_{H2}, Nm	ω_{H2}, s^{-1}	ω_5, s^{-1}	ω_{5-H2}, s^{-1}	P_{fK}, W	ω_{H2fK}, s^{-1}	ɳ, %	Average ɳ, %
10	100,0	100	0	0	100	100	63,4
15	66,7	13,4	-53,3	213,2	52,5	78,7	
20	50,0	-29,9	-79,9	319,6	34,0	68,0	
25	40,0	-56,0	-96	384,0	24,6	61,6	
30	33,3	-73,5	-106,8	427,2	19,1	57,3	
35	28,6	-85,6	-114,2	457,0	15,5	54,3	

M_{H2}, Nm	ω_{H2}, s^{-1}	ω_5, s^{-1}	ω_{5-H2}, s^{-1}	P_{fK}, W	ω_{H2fK}, s^{-1}	ɳ, %	Average ɳ, %
40	25,0	-95,0	-120	480,0	13,0	52,0	
45	22,2	-102,4	-124,6	498,4	11,1	50,2	
50	20,0	-107,9	-127,9	511,6	9,8	48,8	

Based on the data in Table 2, plot the traction characteristic for AD-1 (without additional frictional constraint) as a dependence of the output resistance moment M_{H2} on the output shaft speed ω_{H2fK} (Fig. 4a).

Model №2.

Given: ω_{H1} = 100 s^{-1}, M_{H1} = 10 *Nm*,

M_{H2}= [10, 15, 20, 25, 30, 35, 40, 45, 50] *Nm*,

$\omega_{75} = 50\ s^{-1}$ - average value for preliminary approximate calculation,

z_1 = 40; z_2 = 16; z_3 = 72; z_4 = 16; z_5 = 40; z_6 = 96; z_7 = 20; z_8 = 36.

Determine:

$\omega_5, \omega_7, \omega_{75}, P_f, \omega_{H2f}$ and ɳ.

Solution:

First, the decision is made for AD-2 with a preliminary relative angular velocity $\omega_{75} = const$.

Using Eq. (5) and the output torque data from Table 1, we determine the values of the output angular velocity ω_{H2}.

As an example, determine the value of ω_{H2} at M_{H2} = 10 *Nm* using the following constants:

$P_{H1} = M_{H1}\omega_{H1} = 10 \cdot 100 = 1000\ W$.

$$M_f = -M_{H1}\frac{z_7}{z_8} = -10\frac{20}{36} = -5{,}6\ Nm.$$

$$P_f = |M_f\omega_{75}| = |-5{,}6\text{Нм} \cdot 50\ s^{-1}| = 280\ W.$$

Calculation of the output angular velocity ω_{H2} at M_{H2} = 10 *Nm*:

$$\omega_{H2} = \frac{P_{H1} - P_f}{M_{H2}} = \frac{1000 - 280}{10} = 72\ s^{-1}.$$

Using this solution algorithm, determine the remaining parameters ω_{H2}, which determine the approximate sufficient condition of power adaptation at the corresponding values of M_{H2}. The obtained data are summarized in Table 3.

Table 3: Values of output torque and output angular velocity for AD-2 with an approximately sufficient condition of power adaptation

M_{H2}, Nm	10	15	20	25	30	35	40	45	50
ω_{H2}, s^{-1}	72,0	48,0	36,0	28,8	24,0	20,6	18,0	16,0	14,4

Next, consider the actual operating conditions of the drive.

Model №3.

AD-3 with a real adaptation condition at $\omega_{75} \neq const$.

Using Eqs. (5)…(9), calculate the values of the output angular velocity ω_{H2}.

As an example, below is a numerical calculation for ω_{H2} = 72 s^{-1}.

Let's determine $\omega_5$and ω_7 for all values of ω_{H2}(Table 3) using Eqs. (6) and (7) respectively:

1) For planetary gear at ω_{H2} = 72 s^{-1}:

$$\omega_3 = \frac{\omega_{H2}(1-u_{46}^{H2}) - \omega_{H1}(1-u_{13}^{H1})}{u_{13}^{H1} - u_{46}^{H2}} = \frac{72(1-(-6)) - 100(1-(-1{,}8))}{-1{,}8-(-6)} = 53{,}3\ \text{s}^{-1}.$$

$$\omega_5 = \omega_{H2} + (\omega_3 - \omega_{H2})u_{56}^{H2} = 72 + (53{,}3 - 72) \cdot 2{,}4 = 27{,}1\ \text{s}^{-1}.$$

2) For an additional gear at ω_{H2}= 72 s^{-1}:

$u_{7-H1}^{H2} = -z_8/z_7 = -36/20 = -1{,}8$.

$\omega_7 = \omega_{H2} + (\omega_{H1} - \omega_{H2})u_{7-H1}^{H2} = 72 + (100 - 72) \cdot (-1{,}8) = 21{,}6\ \text{s}^{-1}$.

Determine the variable value of the relative angular velocity ω_{75} by the Eq. (8):

$\omega_{75} = \omega_7 - \omega_5 = 21{,}6 - 27{,}1 = -5{,}5\ \text{s}^{-1}$.

Determine the value of the power for friction P_f using the Eq. (3):

$P_f = |M_f\omega_{75}| = |(-5{,}6) \cdot (-5{,}5)| = 30{,}8\ W$.

Determine the value of the output angular velocity ω_{H2f} using the Eq. (5):

$$\omega_{H2f} = \frac{M_{H1}\omega_{H1} - M_f\omega_{75}}{M_{H2}} = \frac{10 \cdot 100 - 30{,}8}{10} = 96{,}9\ \text{s}^{-1}.$$

Determine the value of efficiency according to the Eq. (9):

$$\eta = \frac{P_{H1}-P_f}{P_{H1}} * 100\% = \frac{1000-30,8}{1000} * 100 = 96,9\%.$$

After performing calculations according to Eqs. (5)...(9), respectively, for each value of M_{H2} and ω_{H2} from Table 3, build Table 4 with the results of calculations ($\omega_5, \omega_7, \omega_{75}, P_f, \omega_{H2f}$ and η) for AD-3 with a real-sufficient condition of power adaptation (there is an additional frictional constraint with a real relative angular velocity).

Table 4: Values of the output torque and output angular velocity for AD-3 with a real-sufficient condition of power adaptation

M_{H2}, s^{-1}	ω_{H2}	ω_5, s^{-1}	ω_7, s^{-1}	ω_{75}, s^{-1}	P_f, W	ω_{H2f}, s^{-1}	η, %	Average η, %
10	72,0	27,1	21,6	-5,5	30,8	96,9	96,9	92,3
15	48,0	-35,3	-45,6	-10,3	57,7	62,8	94,2	
20	36,0	-66,5	-79,2	-12,7	71,1	46,4	92,9	
25	28,8	-85,2	-99,4	-14,2	79,5	36,8	92,1	
30	24,0	-97,7	-112,8	-15,1	84,6	30,5	91,5	
35	20,6	-106,4	-122,3	-15,9	89,0	26,0	91,1	
40	18,0	-113,3	-129,6	-16,3	91,3	22,7	90,9	
45	16,0	-118,4	-135,2	-16,8	94,1	20,1	90,6	
50	14,4	-122,6	-139,7	-17,1	95,8	18,1	90,4	

Based on the data from Table 4, build a graph of the traction characteristic of AD-3 with additional friction coupling in the form of a dependence of the output resistance moment M_{H2} on the output shaft speed ω_{H2f} (Fig. 4b). Figure 4 shows comparative graphs of the characteristics of AD-1 and AD-3.z

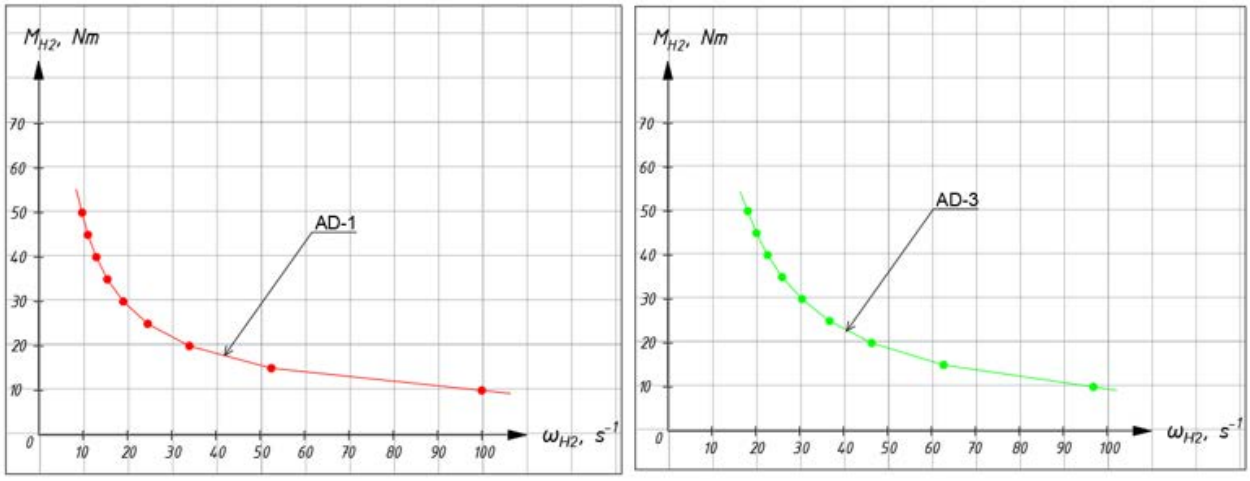

a) b)

Fig. 4. Graphs of the dependence of the output moment of resistance M_(H2)

4a - Graph of the dependence of the output moment of resistance M(H2)on the output angular velocity ω_(H2fK) for AD-1 with a sufficient condition of power adaptation,

4b – Graph of the dependence of the output moment of resistance M(H2)on the output angular velocity ω_(H2f) for AD-3 with a real-sufficient condition of power adaptation.

5 ANALYSIS OF THE RESULTS

Analysis of the obtained results allows us to draw the following conclusions:

1) There is a certainty of the obtained theoretical patterns of the interaction of the parameters of the mechanism. Graph 4b confirms the reliable operation of the developed drive and the presence of the effect of power adaptation;
2) The developed mechanism has a power adaptation of a similar order, high reliability of operation (definability of movement);
3) Model AP-3 has a reliable range of output angular velocity;
4) The efficiency of the AD-3 model is 92% on average, which is much higher than the efficiency of the AD-1 model, which averages 63%;

5) Summarizing points 3 and 4 of the analysis, it can be seen that, compared with the AD-1 model, there was a slight decrease in the control range of the AD-3 model, but at the same time, the efficiency increased significantly.

6 CONCLUSIONS

The performed analysis of the mechanism with two degrees of freedom and with an additional constraint showed a reliable adaptation of the output working body to a variable load. The scheme adopted for the study with an additional balancing constraint in the form of a friction coupling ensures reliable operation and high efficiency of the system.

A slight increase in power losses due to the addition of a friction coupling slightly affects the efficiency and the control range, which remains within a fairly wide range. This is due to the good location of the friction coupling allowing a low relative velocity of the interacting links. Friction coupling creates an efficient force-velocity constraint.

The friction coupling creates an effective force-velocity constraint that replaces the unbalanced reaction and ensures the determinability of movement in a given wide range of regulation.

7 ACKNOWLEDGMENT

This research has been funded by the Science Committee of the Ministry of Higher Education and Science of the Republic of Kazakhstan (Grant No. AP19677356 «To develop systems for controlling the orientation of nanosatellites with flywheels as executive bodies based on linearization methods»).

8 REFERENCES

[1] Kim, D.H.; Kim, J.W.; Choi, S.B. Design and modeling of energy efficient dual clutch transmission with ball-ramp self-energizing mechanism. IEEE Trans. Veh. Technol. 2019, 69, 2525–2536.

[2] Ahssan, M.R.; Ektesabi, M.M.; Gorji, S.A. (2018). Electric vehicle with multi-speed transmission: A review on performances and complexities. SAE Int. J. Altern. Powertrains, 7, 169–182.

[3] Eduardo Louback, Fabricio Machado, Lucas Bruck, Phillip J. Kollmeyer, Ali Emadi (2022). «Real-Time Performance and Driveability Analysis of a Clutchless Multi-Speed Gearbox for Battery Electric Vehicle Applications», IEEE Transportation Electrification Conference & Expo (ITEC), p.1041-1046.

[4] H. Laitinen, A. Lajunen, and K. Tammi (2017). «Improving electric vehicle energy efficiency with two-speed gearbox», in Proc. IEEE Veh. Power Propulsion Conf., Apr., p. 1–5.

[5] T. Hofman and C. H. Dai (2011). «Energy efficiency analysis and comparison of transmission technologies for an electric vehicle», in Proc. IEEE Veh. Power Propulsion Conf., p. 23–28.

[6] A. Sorniotti, S. Subramanyan, A. Turner, C. Cavallino, F. Viotto, and S. Bertolotto (2011). «Selection of the optimal gearbox layout for an electric vehicle», SAE Int. J. Engines, vol. 4, no. 1, p. 1267–1280.

[7] Q. Ren, D. A. Crolla, and A. Morris (2009), «Effect of transmission design on electric vehicle (EV) performance», in Proc. IEEE Veh. Power Propulsion Conf., p. 1260–1265.

[8] B. Eberleh and T. Hartkopf (2006). «A high-speed induction machine with two speed transmission as drive for electric vehicles», in Proc. Int. Symp. Power Electron., Elect. Drives, Automat. Motion, p. 249–254.

[9] F. A. Machado, P. J. Kollmeyer, D. G. Barroso and A. Emadi (2021). «Multi-speed gearboxes for battery electric vehicles: Current status and future trends», IEEE Open Journal of Vehicular Technology, vol. 2, p. 419-435.

[10] J. Ruan, P. D. Walker, J. Wu, N. Zhang, and B. Zhang (2018). «Development of continuously variable transmission and multi-speed dual-clutch transmission for pure electric vehicle», Adv. Mech. Eng., vol. 10, no. 2, p. 1–15.

[11] Jianjun Hu, Feng Xiao, Hang Peng, Wei Zhao (2022). CVT discrete speed ratio optimizations based on energy efficiency for PHEV. Alexandria Engineering Journal, vol. 61, issue 5, p. 4095-4105.

[12] Mantriota G, Reina G. (2021). Dual-Motor Planetary Transmission to Improve Efficiency in Electric Vehicles. Machines, 9, 58.

[13] Meng, D.; Wang, F.; Wang, Y.; Gao, B. (2021). In-Wheel Two-Speed AMT with Selectable One-Way Clutch for Electric Vehicles. Actuators, 10, 220.

[14] Ivanov K.S., Yaroslavceva E.K.: Transmission and device for changing the torque and output speed depending on the resistance to movement, Germany. Patent No. 21 2018 000 129.

[15] Ivanov K.S. (2021). Theory of adaptive mechanical drive. Theoretical and Applied Mechanics Letters. Elsevier, vol. 11, issue 4, 1 – 5.

Paper submitted: 13.06.2023.

Paper accepted: 08.03.2024.